Magnetic Ordering-Induced Multiferroic Behavior in [CH₃NH₃][Co(HCOO)₃] Metal−Organic Framework

L. Claudia Gómez-Aguirre,*,†,‖ Breogán Pato-Doldán,†,‖,⊥ J. Mira,‡ Socorro Castro-García,†
María Antonia Señarís-Rodríguez,† Manuel Sánchez-Andújar,† John Singleton,§ and Vivien S. Zapf*,§

†Department of Fundamental Chemistry, Faculty of Sciences, University of A Coruña, 15071 A Coruña, Spain
‡Department of Applied Physics, University of Santiago de Compostela, 15782 Santiago de Compostela, Spain
§National High Magnetic Field Laboratory, Los Alamos National Laboratory, Los Alamos, New Mexico 87545, United States

S *Supporting Information*

ABSTRACT: We present the first example of magnetic ordering-induced multiferroic behavior in a metal−organic framework magnet. This compound is [CH₃NH₃][Co-(HCOO)₃] with a perovskite-like structure. The A-site [CH₃NH₃]⁺ cation strongly distorts the framework, allowing anisotropic magnetic and electric behavior and coupling between them to occur. This material is a spin canted antiferromagnet below 15.9 K with a weak ferromagnetic component attributable to Dzyaloshinskii− Moriya (DM) interactions and experiences a discontinuous hysteretic magnetic-field-induced switching along [010] and a more continuous hysteresis along [101]. Coupling between the magnetic and electric order is resolved when the field is applied along this [101]: a spin rearrangement occurs at a critical magnetic field in the ac plane that induces a change in the electric polarization along [101] and [10-1]. The electric polarization exhibits an unusual memory effect, as it remembers the direction of the previous two magnetic-field pulses applied. The data are consistent with an inverse-DM mechanism for multiferroic behavior.

Magnetoelectric multiferroics materials, in which magnetic and electric orders coexist and are coupled,[1−4] have been the subject of extensive research due to their potential applications in devices that can sense and create magnetic polarizations using electric fields and vice versa.[5,6] These properties are usually investigated in transition-metal oxides. However, recently the research has been extended to metal− organics[7−9] and in particular metal−organic frameworks (MOFs),[10−12] which provide a different approach to multiferroic behavior, due to their modular designable nature.

MOFs are ordered crystalline structures composed of porous frameworks of inorganic metal ions connected by organic linkers and guest cations within the pores. Among the MOFs with shorter linkers and denser structures, long-range magnetic and electric order can emerge. The series [amineHₙ][M(HCOO)₃], where M²⁺ is a transition-metal ion and [amineHₙ]⁺ is a protonated amine, are promising multiferroic type I materials.[10,11,13−16] In these compounds the magnetic and ferroelectric orders have different origins: The ferroelectric order is associated with order/disorder transitions of the [amineHₙ]⁺ cations, while magnetism originates from the framework [M(HCOO)₃]⁻. More recently, a coupling between magnetic and electric order has been predicted in this family of compounds[17−20] and reported experimentally in the paramagnetic state of [(CH₃)₂NH₂][Mn(HCOO)₃] associated with the ferroelectric transition[21] and in [(CH₃)₂NH₂][Fe(HCOO)₃],[22] where the dielectric anomaly observed at the magnetic ordering temperature can be suppressed by external magnetic fields.

Here, we demonstrate for the first time electric polarization induced entirely by magnetic ordering (type II multiferroic behavior), at a field-induced magnetic transition in a perovskite-like MOF, [CH₃NH₃][Co(HCOO)₃] ("Co-MOF").

Well-faceted mm-sized Co-MOF single crystals (Figure S1) as well as polycrystals were prepared by solvothermal reaction of a stoichiometric mixture of methylammonium chloride, sodium formate, and cobalt chloride in water/methylformamide (details in SI) as described for analogue MOFs of formula [(CH₃)₂NH₂]-[M(HCOO)₃].[23]

The obtained material is single phase, as indicated by X-ray powder diffraction (Figure S2). The thermal analysis indicates that it is chemically stable up to 488 K (Figure S3). Above this temperature the decomposition process occurs in two steps. A combination of CoO and Co was identified as final product of its thermal decomposition at 873 K (Figure S4). Single-crystal X-ray diffraction studies carried out at 100 K reveal an orthorhombic structure with space-group *Pnma* (*Z* = 4). The structural data are summarized in Table S1 and are consistent with previously reports[24] at 300 K.

The Co-MOF compound has a distorted perovskite-like structure (Figure 1) where the asymmetric unit contains one independent metal Co²⁺ cation, two HCOO⁻ formate groups, and one methylammonium, CH₃NH₃⁺ cation (MA). Each Co²⁺ is connected to its six metal nearest neighbors through anti−anti bridging HCOO⁻ anions in a slightly distorted octahedral environment with three different Co−O bond lengths. The "pseudo" cubooctahedral cavities are occupied by the MA cations, which lie parallel to the ac plane along the [103] and [10-3] directions. In such cavities, each N atom is linked to three formate ligands of the framework: (i) through two linear and stronger N−H···O hydrogen bonds within the ac plane and (ii) through one bifurcated and weaker H-bond along the *b*-axis (see
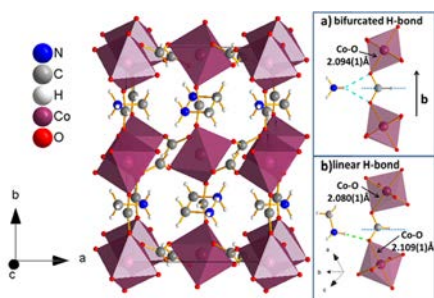
Figure 1. Crystal structure of Co-MOF at 100 K. Inset: Details of the H-bonds between the MA cation and the framework (a) along b, where the two O atoms of the formate ligands are involved in a weak bifurcated H-bond, and (b) parallel to the ac plane, where only one of the two O atoms of the formate ligand is involved in a strong linear H-bond.
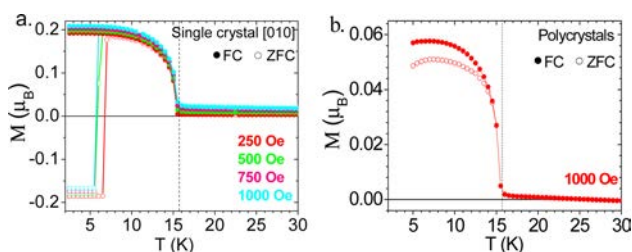

Figure 2. Zero-field cooled (ZFC) and field cooled (FC) magnetization M as a function of temperature measured with different magnetic fields in (a) a single crystal of Co-MOF oriented with $M\|H\|[010]$ and (b) a polycrystalline sample.

details in Figure 1). As a result, the $[Co(HCOO)_3]^-$ framework displays a distortion: (i) within the ac plane as only one of the two O atoms of each formate is involved in a strong linear H-bond, leading two different Co−O bond lengths and shifting each formate out of the middle position between the two cobalt atoms; and (ii) along the b-axis, where the two O atoms of each formate are involved in a weak bifurcated H-bond, leading two equal Co−O bond lengths and formate ligands centered between two cobalt atoms. We highlight, consequently, the effect of the H-bonds on the $[Co(HCOO)_3]^-$ framework distortions, mainly observed in the ac plane, where the H-bonds are stronger.

The magnetic properties of Co-MOF were investigated in poly and single crystals. Magnetization measurements were performed in a vibrating sample magnetometer of a 14 T physical properties measurement (PPMS) system (Figures 2a and S5) and in a SQUID in a 5 T PPMS (Figure 2b). These data are consistent with antiferromagnetic ordering with a weak ferromagnetic component below 15.9 K due to spin canting, similar to that reported for analogue formates[23,25] (Table S2). Negative magnetization upon "zero"-field cooling observed along $[010]$ (Figure 2a) is attributed to the negative trapped flux in the superconducting magnet: ∼1 Oe in the 5 T magnet and ∼10 Oe in the 14 T magnet after oscillating the field to zero prior to a "zero"-field cool. The presence of a remnant field in the magnet is compounded by the unusual fact that the majority of this sample's low-temperature magnetization along $[010]$ is independent of field used to cool it, between 10 and 1000 Oe. Thus, the magnetization approaches a value of ∼0.19 μ_B at low temperatures rather than zero, as the field in which it is cooled is lowered toward zero. We will discuss later that this is not consistent with ordinary magnetic domain behavior in ferromagnets.[26] Measurements in a polycrystalline sample show that Co-MOF obeys the Curie−Weiss law above 20 K
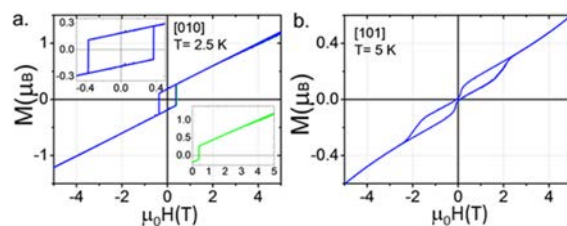

Figure 3. Field-dependent isothermal magnetization $M(T, \mu_0 H)$ for Co-MOF with M and H along (a) $[010]$ at 2.5 K. Insets show zoomed views of the magnetic hysteresis (blue) and initial magnetization curve (green) (b) $[101]$ at 5 K.
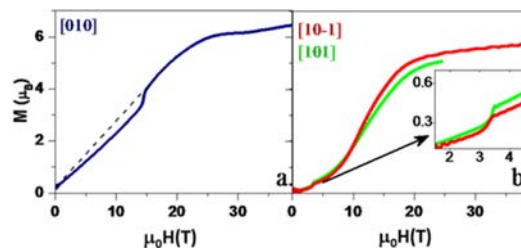

Figure 4. Pulsed-field magnetization of Co-MOF along (a) $[010]$ and (b) $[101]$ and $[10\text{-}1]$ orientations at T = 4 K. The inset highlights the magnetization jump observed near 3.5 T.

(Figure S6) with C = 3.45 cm^{3}K/mol, μ_{eff} = 5.23 μ_B, and θ = −43.5 K. As usually observed, the effective magnetic moment of the Co^{2+} ion is higher than expected for a spin-only value (S = 3/2, μ_{eff} = 3.88 μ_B) due to a small unquenched orbital component.

Isothermal magnetization measurements carried out on a single crystal with fields up to 5 T show a square hysteresis loop with a coercive field of 0.4 T and a remnant magnetization of 0.19 μ_B when the crystal is oriented along the $[010]$ direction (Figures 3a and S7). Measurements as a function of H and T (Figure S7) reveal sudden discontinuous switching. Meanwhile, for $H\|[101]$ (Figures 3b and S8), $M(\mu_0 H)$ shows a gradual, wasp-waisted hysteresis loop with no remnant moment at H = 0 (see SI for other temperatures down to 2 K). A similar $M(\mu_0 H)$ behavior is found for fields applied along the $[10\text{-}1]$ direction.

Capacitor-driven pulsed magnets with a few millisecond rise time were used to measure magnetization to 65 T by recording the induced current in a compensated coil (see SI). The $M(\mu_0 H)$ results along the three orientations of the crystal at similar temperatures (≈4 K) are shown in Figure 4 for upsweeps of the magnetic field. From the magnitude of M, $[010]$ is the magnetic easy axis below 10 T. Also, $M(\mu_0 H)$ along $[010]$ reveals an additional jump at 14.5 T, which is consistent with a spin flop, since it occurs along the easy axis, and magnetization above 14.5 T can be linearly extrapolated back to the origin (dashed line in Figures 4a and S9).

In the pulsed-field $M(\mu_0 H)$ curves for $H\|[101]$ and $[10\text{-}1]$ (Figure 4b), the transition that occurred in the superconducting magnet measurements (Figure 3b) is reproduced at similar fields (see Figures S8 and S10). The magnetization starts to saturate near 26 T for $[010]$ (Figure 4a) and 21 T for $[101]$ and $[10\text{-}1]$ (Figure 4b). A magnetization value near 6 μ_B achieved by 40 T is consistent with Co^{2+} cations with unquenched orbital-moment.

The change in the electric polarization of Co-MOF was measured upon application of a magnetic field for combinations of P and H along $[101]$, $[10\text{-}1]$, and $[010]$.[27−31] Capacitor plates were created on parallel surfaces with silver paint. The induced current I_{ME} due to the changing surface charge was measured in
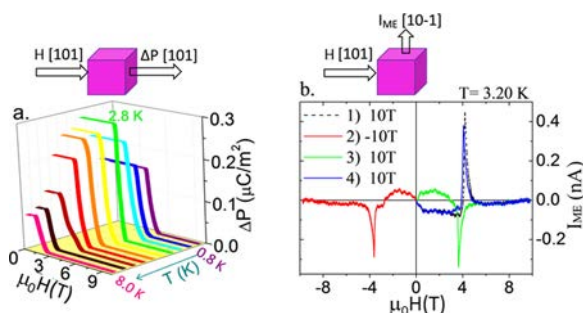
Figure 5. (a) Change in electric polarization, $\Delta P = P(\mu_0 H) - P(H = 0)$ along [101] measured for increasing $H \| [101]$ at different temperatures. (b) Raw magnetoelectric current, I_{ME}, along [10-1] at 3.2 K for a series of positive and negative magnetic-field pulses applied along [101], and which almost overlap in the case of the blue and black line.

capacitor-driven millisecond magnetic-field pulses, and integrated to extract the change in electric polarization $\Delta P = P(H) - P(H = 0)$. Pulsed magnets with 10^3 T/s sweep rates were used to enhance the resolution compared to measurements in superconducting magnets with 10^{-2} T/s sweep rates.[8,29,32−34]

As can be seen in Figure 5a,b, a sharp change in the electric polarization occurs when a pulsed magnetic field is applied along [101] and ΔP is measured along [101] or [10-1]. A sharp polarization decrease occurs when the applied magnetic field reaches a critical value. For example, for $T = 2.8$ K, a decrease in ΔP from a value of 0.28 $\mu C/m^2$ occurs for $\mu_0 H \geq H_{crit} \sim 4$ T, which corresponds to the kink observed in the $M(\mu_0 H)$ curves along [101] and [10-1] directions (Figures S10 and S11).

Another interesting finding is that the direction of the electric polarization can be switched depending on the history of the previous two magnetic-field pulses. In Figure 5b, we show the magnetoelectric current (time derivative of the electric polarization) measured along [10-1], I_{ME}, for the upsweep of a series of magnetic-field pulses applied in positive and negative direction along [101] (more details in SI). When two consecutive magnetic-field pulses are applied in the indicated opposite directions (black and red lines), the resulting I_{ME} is negative (red line) along [10-1]. On the other hand, when two consecutive pulses are applied along the same direction (green and blue lines), the resulting I_{ME} is "positive" (blue line). Note that in Figure 5a the jumps ΔP are all shown as positive. This transverse "memory effect" is unusual but similar to one previously reported for copper dimethyl sulfoxide dichloride (CDC), where it is related to DM effects.[8]

Putting all this information together, we attribute the kink in the magnetization at ∼3.5 T, correlating to a jump in electric polarization, to a magnetic-field-induced change in magnetic ordering, that also changes the spatial-inversion symmetry breaking and thereby alters ferroelectricity.[27,28,30,31,33] In particular, magnetic ordering involving an inverse-DM effect is known to be a mechanism for producing electric polarization coupled to a transverse magnetization, while DM interactions can produce canted antiferromagnetism with a small remnant magnetization as we observe here.[35] The DM interaction results from canted bonds where a charged negative ion between two positive ones has been displaced off-center perpendicular to the bond axis. This produces an electric dipole as well as a spin−orbit interaction that favors a noncollinear alignment of the spins and therefore a small net magnetic moment in an antiferromagnetic state. The alternating canted $[Co(HCOO)_3]^-$ bonds created by interaction with the MA guest cation in the Co-MOF structure

could support a weak ferromagnetism within the antiferromagnetic state due to a DM mechanism. However, the room-temperature structure in this material does not support a net electric polarization since the electric dipoles of different canted bonds in the structure cancel each other out. In the inverse-DM mechanism for multiferroic behavior, a subtle structural distortion occurs in the magnetically ordered state that breaks overall spatial inversion symmetry such that electric dipoles on different canted bonds no longer cancel each other out, creating ferroelectricity.[36] Finally, the electrically polar MA guest cations, although arranged antiferroelectrically at room temperature, are bonded to the formate group in the canted bonds and thereby should respond to the distorted structure in the ferroelectric state and contribute additional electric polarization. In other family members of these hybrid perovskites, it is known that H-bonding of the guest cation to the formate groups couples to magnetic exchange.[37]

Finally the origin of the magnetic switching in this compound is unlikely to be due to traditional domain switching. Domain formation favors a zero-field-cooled magnetization with no net magnetic moment,[26] whereas here a persistent moment of ∼0.19 μ_B remains along [010] even as the field in which we cool through the ordering temperature is reduced from 1 kOe to 10 Oe. The small size of the moment may be insufficient to trigger domain formation, relative to the energy cost of creating domain boundaries. Regarding the "wasp-waisted" hysteresis loop along [101], it has the appearance of a field-induced magnetic phase transition that is hysteretic between up and down sweeps.

The obtained magnetic and electric information for this single crystal Co-MOF is summarized in the magnetic field−temperature phase diagrams we have constructed for the [010] and [101]/[10-1] directions (Figure 6a,b, respectively) and reflects the anisotropic magnetism and magnetoelectric coupling displayed by this $[CH_3NH_3][Co(HCOO)_3]$ compound below 15.9 K.
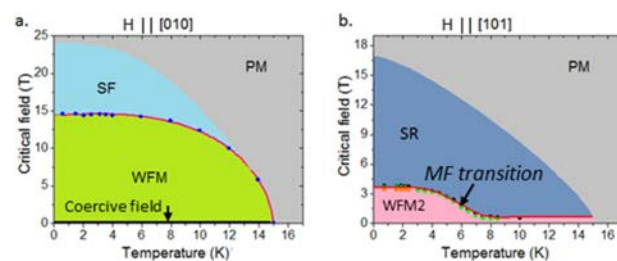

Figure 6. Phase diagram of Co-MOF for H along (a) [010] and (b) [101] with data points extracted from peaks in the field derivative of the magnetization and electric polarization data, and the crossover to paramagnetism is estimated from the peak in d^2M/dH^2 at magnetic saturation (details in SI). MF is the multiferroic transition. Color code, green, pink: weak ferromagnetic (WFM, WFM2), light blue: spin-flop (SF), dark blue: spin rearrangement (SR), gray: paramagnetic (PM).

In conclusion, we present a rare example of a MOF with coupled magnetic and electric order. This $[CH_3NH_3][Co(HCOO)_3]$ compound, with perovskite-like structure, presents a weak ferromagnetic component due to spin canting below 15.9 K attributable to DM interactions with a discontinuous hysteretic magnetic-field-induced switching along [010] and a more continuous hysteresis along [101] coupled to a parallel and transverse electric polarization along [101] and [10-1], respectively. An inverse DM mechanism could be responsible for the electric polarization. An additional spin-flop transition is

observed at 14.5 T along [010], which evolves with temperature. Furthermore, the electric polarization along [101] and [10-1] for fields along [101] exhibits a memory effect that remembers the direction of the previous two magnetic-field pulses.

This Co-MOF constitutes the first example of ferroelectricity induced by magnetic order in MOFs and thus opens this large, flexible, multifunctional and designable family of compounds to magnetically-induced multiferroic behavior. We expect that this discovery will lead to continued efforts to understand the precise spin structure that is creating the symmetry breaking necessary to induce ferroelectric behavior and to modify this material to enhance the effect and the critical temperatures.

■ ASSOCIATED CONTENT

Ⓢ Supporting Information
The Supporting Information is available free of charge on the ACS Publications website at DOI: 10.1021/jacs.5b11688.

Crystallographic data (CIF)
Experimental details and data (PDF)

■ AUTHOR INFORMATION

Corresponding Authors
*vzapf@lanl.gov
*claudia.gomez.aguirre@udc.es

Present Address
⊥University of Bergen, P.O. Box 7803, N-5020 Bergen, Norway.

Author Contributions
‖These authors contributed equally.

Notes
The authors declare no competing financial interest.

■ REFERENCES

(1) Spaldin, N. A.; Fiebig, M. *Science* **2005**, *309*, 391.
(2) Eerenstein, W.; Mathur, N. D.; Scott, J. F. *Nature* **2006**, *442* (7104), 759.
(3) Hill, N. A. *J. Phys. Chem. B* **2000**, *104* (29), 6694.
(4) Khomskii, D. *Physics* **2009**, *2*, 1.
(5) Scott, J. F. *Nat. Mater.* **2007**, *6* (4), 256.
(6) Chu, Y.-H.; Martin, L. W.; Holcomb, M. B.; Gajek, M.; Han, S.-J.; He, Q.; Balke, N.; Yang, C.-H.; Lee, D.; Hu, W.; Zhan, Q.; Yang, P.-L.; Fraile-Rodríguez, A.; Scholl, A.; Wang, S. X.; Ramesh, R. *Nat. Mater.* **2008**, *7* (6), 478.
(7) Polyakov, A. O.; Arkenbout, A. H.; Baas, J.; Blake, G. R.; Meetsma, A.; Caretta, A.; Van Loosdrecht, P. H. M.; Palstra, T. T. M. *Chem. Mater.* **2012**, *24*, 133.
(8) Zapf, V. S.; Kenzelmann, M.; Wolff-Fabris, F.; Balakirev, F.; Chen, Y. *Phys. Rev. B: Condens. Matter Mater. Phys.* **2010**, *82*, 060402(R).
(9) Zapf, V. S.; Sengupta, P.; Batista, C. D.; Nasreen, F.; Wolff-Fabris, F.; Paduan-Filho, A. *Phys. Rev. B: Condens. Matter Mater. Phys.* **2011**, *83*, 140405.
(10) Xu, G.-C.; Zhang, W.; Ma, X.-M.; Chen, Y.-H.; Zhang, L.; Cai, H.-L.; Wang, Z.-M.; Xiong, R.-G.; Gao, S. *J. Am. Chem. Soc.* **2011**, *133* (38), 14948.
(11) Jain, P.; Ramachandran, V.; Clark, R. J.; Zhou, H. D.; Toby, B. H.; Dalal, N. S.; Kroto, H. W.; Cheetham, A. K. *J. Am. Chem. Soc.* **2009**, *131* (38), 13625.
(12) Zhang, W.; Xiong, R.-G. *Chem. Rev.* **2012**, *112* (2), 1163.
(13) Rogez, G.; Viart, N.; Drillon, M. *Angew. Chem., Int. Ed.* **2010**, *49* (11), 1921.
(14) Sánchez-Andújar, M.; Presedo, S.; Yáñez-Vilar, S.; Castro-García, S.; Shamir, J.; Señarís-Rodríguez, M. A. *Inorg. Chem.* **2010**, *49* (4), 1510.
(15) Pato-Doldán, B.; Gómez-Aguirre, L. C.; Bermúdez-García, J. M.; Sánchez-Andújar, M.; Fondado, A.; Mira, J.; Castro-García, S.; Señarís-Rodríguez, M. A. *RSC Adv.* **2013**, *3* (44), 22404.
(16) Fu, D.-W.; Zhang, W.; Cai, H.-L.; Zhang, Y.; Ge, J.-Z.; Xiong, R.-G.; Huang, S. D.; Nakamura, T. *Angew. Chem., Int. Ed.* **2011**, *50* (50), 11947.
(17) Di Sante, D.; Stroppa, A.; Jain, P.; Picozzi, S. *J. Am. Chem. Soc.* **2013**, *135* (48), 18126.
(18) Stroppa, A.; Jain, P.; Barone, P.; Marsman, M.; Perez-Mato, J. M.; Cheetham, A. K.; Kroto, H. W.; Picozzi, S. *Angew. Chem., Int. Ed.* **2011**, *50* (26), 5847.
(19) Stroppa, A.; Barone, P.; Jain, P.; Perez-Mato, J. M.; Picozzi, S. *Adv. Mater.* **2013**, *25* (16), 2284.
(20) Tian, Y.; Cong, J.; Shen, S.; Chai, Y.; Yan, L.; Wang, S.; Sun, Y. *Phys. Status Solidi RRL* **2014**, *8* (1), 91.
(21) Wang, W.; Yan, L.-Q.; Cong, J.-Z.; Zhao, Y.-L.; Wang, F.; Shen, S.-P.; Zou, T.; Zhang, D.; Wang, S.-G.; Han, X.-F.; Sun, Y. *Sci. Rep.* **2013**, *3*, 2024.
(22) Tian, Y.; Stroppa, A.; Chai, Y.; Yan, L.; Wang, S.; Barone, P.; Picozzi, S.; Sun, Y. *Sci. Rep.* **2014**, *4*, 6062.
(23) Wang, X.-Y.; Gan, L.; Zhang, S.-W.; Gao, S. *Inorg. Chem.* **2004**, *43* (15), 4615.
(24) Boča, M.; Svoboda, I.; Renz, F.; Fuess, H. *Acta Crystallogr., Sect. C: Cryst. Struct. Commun.* **2004**, *60* (12), m631.
(25) Hu, K.-L.; Kurmoo, M.; Wang, Z.; Gao, S. *Chem. - Eur. J.* **2009**, *15* (44), 12050.
(26) Cullity, B. D.; Graham, C. D. *Introduction to Magnetic Materials*; John Wiley & Sons, Inc.: Hoboken, NJ, 2008.
(27) Kimura, T.; Goto, T.; Shintani, H.; Ishizaka, K.; Arima, T.; Tokura, Y. *Nature* **2003**, *426* (6962), 55.
(28) Aliouane, N.; Argyriou, D. N.; Strempfer, J.; Zegkinoglou, I.; Landsgesell, S.; Zimmermann, M. v. *Phys. Rev. B: Condens. Matter Mater. Phys.* **2006**, *73*, 020102.
(29) Kim, J. W.; Artyukhin, S.; Mun, E. D.; Jaime, M.; Harrison, N.; Hansen, A.; Yang, J. J.; Oh, Y. S.; Vanderbilt, D.; Zapf, V. S.; Cheong, S.-W. *Phys. Rev. Lett.* **2015**, *115*, 137201.
(30) Kim, J. W.; Kamiya, Y.; Mun, E. D.; Jaime, M.; Harrison, N.; Thompson, J. D.; Kiryukhin, V.; Yi, H. T.; Oh, Y. S.; Cheong, S.-W.; Batista, C. D.; Zapf, V. S. *Phys. Rev. B: Condens. Matter Mater. Phys.* **2014**, *89*, 060404.
(31) Mun, E. D.; Chern, G.-W.; Pardo, V.; Rivadulla, F.; Sinclair, R.; Zhou, H. D.; Zapf, V. S.; Batista, C. D. *Phys. Rev. Lett.* **2014**, *112*, 017207.
(32) Mun, E.; Wilcox, J.; Manson, J. L.; Scott, B.; Tobash, P.; Zapf, V. S. *Adv. Condens. Matter Phys.* **2014**, *2014*, 512621.
(33) Lin, S.-Z.; Barros, K.; Mun, E.; Kim, J.-W.; Frontzek, M.; Barilo, S.; Shiryaev, S. V.; Zapf, V. S.; Batista, C. D. *Phys. Rev. B: Condens. Matter Mater. Phys.* **2014**, *89*, 220405.
(34) Oh, Y. S.; Artyukhin, S.; Yang, J. J.; Zapf, V.; Kim, J. W.; Vanderbilt, D.; Cheong, S.-W. *Nat. Commun.* **2014**, *5*, 3201.
(35) Wang, K. F.; Liu, J.-M.; Ren, Z. F. *Adv. Phys.* **2009**, *58* (4), 321.
(36) Sergienko, I. A.; Dagotto, E. *Phys. Rev. B: Condens. Matter Mater. Phys.* **2006**, *73*, 094434.
(37) Tian, Y.; Wang, W.; Chai, Y.; Cong, J.; Shen, S.; Yan, L.; Wang, S.; Han, X.; Sun, Y. *Phys. Rev. Lett.* **2014**, *112*, 017202.